Exploring Grainyhead-like 2 target genes in breast cancer

Wang, Z.

Chapter 2

The role of GRHL2 in luminal- and basal like breast cancer

Zi Wang[1], Bircan Coban[1], Chen-Yi Liao[1], Yao-Jun Chen[1], Erik HJ Danen[1, *]

[1]Division of Drug Discovery and Safety, Leiden Academic Center for Drug Research, Leiden University, The Netherlands

* Corresponding author: Erik HJ Danen; e.danen@lacdr.leidenuniv.nl; Division of Drug Discovery and Safety, Leiden Academic Center for Drug Research, Leiden University, Einsteinweg 55, 2333CC Leiden, The Netherlands

Abstract

The transcription factor Grainyhead like 2 (GRHL2) is reported to promote cancer growth in some-, and suppress aspects of cancer progression in other studies. We investigated its role in different breast cancer subtypes. In breast cancer patients, association of GRHL2 expression with prognosis differed for different subtypes and in a large cell line panel, GRHL2 was low or absent in basal B- and expressed in all luminal- and basal A cell lines. In a luminal cell line (MCF7) deletion of GRHL2 triggered cell cycle arrest, loss of colony formation capacity, and downregulation of PCNA and TERT. In parallel, E-cadherin was lost but only a minor increase in EGF-stimulated motility was observed. In a basal A cell line (HCC1806) GRHL2 deletion also suppressed proliferation and colony formation but no changes were seen in PCNA and TERT. Rather, loss of E-cadherin in this case was accompanied by induction of Vimentin and N-cadherin, and conversion to a highly migratory phenotype, further augmented by EGF treatment. These results point to distinct responses to GRHL2 depletion in luminal- and basal-like breast cancers with respect to growth arrest and enhanced motility phenotypes and suggest that GRHL2 may be a candidate target in luminal-like breast cancer.

Introduction

Breast cancer is the most prevalent malignancy in female globally. Mortality of patients with breast cancer has decreased, resulting from early diagnosis and development of therapies [1-3]. A considerable proportion of knowledge on breast cancer originates from experiments performed with breast cancer cells that cover the various subtypes of this heterogeneous disease [4]. Breast cancer is divided into luminal-like (luminal A and luminal B), epidermal growth factor receptor 2-enriched (HER2-enriched), basal-like (basal A and basal B), claudin-low, and normal-like subtypes based on gene expression profiling [5].

Luminal-like breast cancer is characterized by enrichment of genes/proteins associated with the luminal epithelial phenotype (e.g., ESR1, GATA3 and FOXA1) [4,6]. Basal-like breast cancer is characterized by significant enrichment of basal epithelial cytokeratins, hormone receptor negativity and a high tumor grade and poor prognosis

[7]. Basal-like breast cancer can be further divided into basal A and basal B subtype [8]. The basal A subtype is enriched with basal markers such as cytokeratins, while basal-B exhibits a mesenchymal or a normal-like phenotype with overexpression of several genes related to tumor invasion and tumor stemness [4].

The Grainyhead (*GRH*) gene was originally discovered through a mutation that causes slack and fragile cuticles in *Drosophila*[9]. This gene mutation results in failure of neural tube closure during embryogenesis [10]. The transcription factor GRH family is highly conserved from *Drosophila* to humans. In humans, GRHL1, GRHL2 and GRHL3 are identified as GRH homologs that contain an N-terminal transcriptional activation domain, a central CP2 DNA-binding domain and a C-terminal dimerization domain [11].

GRHL2 has been implicated in cancer development. In some studies, GRHL2 is considered as a tumor suppressor, because it suppresses epithelial-mesenchymal transition (EMT) through upregulation of epithelial markers or downregulation of mesenchymal markers [12-14]. In contrast, *GRHL2* is located on chromosome 8q22 that is frequently amplified or overexpressed in many cancers and hence may rather have an oncogenic function [15]. Indeed, in prostate cancer [16], breast cancer [14], lung cancer [17] and ovarian cancer [18] downregulation of GRHL2 has been associated with inhibition of cell proliferation. Together, this suggests that GRHL2 function may vary depending on the cancer cell context.

In this study, we investigated the role of GRHL2 in different breast cancer subtypes. Our findings show that GRHL2 is absent in basal B-like breast cancer cells, it is expressed in basal A where its deletion triggers a slow growth/high motility phenotype, and it is expressed in luminal-like breast cancer cells where its depletion causes an arrested replication/proliferation.

Materials and methods

Cell lines

Human breast cancer cell lines (MCF7, T47D, BT474, HCC1806, BT20, MDA-MB-468, Hs578T) were obtained from the American Type Culture Collection. Cells were cultured

in RPMI1640 medium with 10% fetal bovine serum, 25 U/mL penicillin and 25 µg/mL streptomycin in the incubator (37°C, 5% CO_2).

For production of lentiviral particles, VSV, GAG, REV and Cas9 or sgRNA plasmids were transfected into HEK293 cells using Polyethylenimine (PEI). After 2 days, lentiviral particles were harvested and filtered. Conditional Cas9 cells were generated by infecting parental cells with lentiviral particles expressing Edit-R Tre3G promotor-driven Cas9 (Dharmacon) and selected by blasticidin. Limited dilution was used to generate Cas9 monoclonal cells. Subsequently, Cas9-monoclonal cells were transduced with U6-gRNA:hPGK-puro-2A-tBFP control non-targeting or GRHL2-specific single guide (sg)RNAs (Sigma) and selected by puromycin.

Western blot

Cells were lysed by radioimmunoprecipitation (RIPA) buffer (150 mM NaCl, 1% Triton X-100, 0.5% sodium deoxycholate and 0.1% Tris and 1% protease cocktail inhibitor (Sigma-Aldrich. P8340)). Then cell lysis was sonicated and protein concentration was determined by bicinchoninic acid assay (BCA) assay. Cell lysis was mixed with protein loading buffer. Subsequently, protein was separated by SDS-PAGE gel and then transferred to methanol-activated polyvinylidene difluoride (PVDF) (Milipore, The Netherlands) membrane. The membrane was blocked with 5% bovine serum albumin (BSA, Sigma-Aldrich) for 1 hour at room temperature (RT). Then membranes were stained with primary antibody overnight at 4°C and HRP-conjugated secondary antibodies for half hour at room temperature (RT). After staining with Prime ECL Detection Reagent (GE Healthcare Life science), chemoluminescence was detected by Amersham Imager 600 (GE Healthcare Life science, The Netherlands). The following antibodies were used: GRHL2 (Atlas-Antibodies, hpa004820), GAPDH (SantaCruz, sc-32233), PCNA (SantaCruz, sc-56), Vimentin (Abcam, ab8069), N-cadherin (BD, 610920), E-cadherin (Abcam, ab76055), Peroxidase AffiniPure Goat Anti-Rabbit IgG (Jackson ImmunoResearch, 111-035-003), Peroxidase AffiniPure Goat Anti-Mouse IgG (Jackson ImmunoResearch, 115-035-003). Original blots are shown in Supplementary Figures.

Sulforhodamine B (SRB) assay

Cell proliferation rate was measured by SRB assay. Cells were seeded into 96-well plates. At indicated time points, cells were fixed with 50% Trichloroacetic acid (TCA, Sigma-Aldrich) for 1 hour at 4 °C and then plates were washed with demineralized water four times and air-dried at RT. Subsequently, 0.4% SRB (60 µl/well) was added and kept for at least 2 hours at RT. The plates were washed five times with 1% acetic acid and air-dried. 10 mM (150 µl/well) Tris was added and kept for half hour at RT with gentle shaking. The absorbance value was measured by a plate-reader Fluostar OPTIMA.

Realtime quantitative PCR (RT-qPCR)

Total RNA was isolated using RNEasy Plus Mini Kit (Qiagen). 500 ng RNA was reverse-transcribed into cDNA using the RevertAid H Minus First Strand cDNA Synthesis Kit (Thermo Fisher Scientific). The cDNA was mixed with SYBR green master mix (Fisher Scientific) for qPCR. RT-qPCR data were collected and analyzed using $2^{-\Delta\Delta Ct}$ method. The primers are shown in supplementary table 1.

Immunofluorescence

Cells were fixed with 2% formaldehyde for 15 minutes under slow rotation, permeabilized with 1% Triton in Phosphate buffered saline (PBS) for 10 minutes, and then stained with primary antibodies and secondary antibodies. The following antibodies were used: Vimentin (Abcam, ab8069); E-cadherin (Abcam, ab76055); Hoechst (33258, Abcam); β-catenin (BD, 610153); Goat anti-Mouse IgG (H+L) Cross-Adsorbed Secondary Antibody-Alexa Fluor 488 (Thermo Fisher, A-11001); Rhodamine-Phalloidin (Thermo Fisher, R415).

Three-dimensional (3D) culture

Collagen (2 mg/ml, 70 µl/well) was added into 96-well plates. Plates were kept in the incubator (37°C, 5% CO_2) for 1 hour. A subconfluent layer of cells in a T25 flask was detached by 0.25% trypsin and collected. The cell suspension was centrifuged at 230×g for 5 minutes. The cell pellet was resuspended in 50 µl 2% Polyvinylpyrrolidone. The cell suspension was injected into the collagen scaffolds to generate ~200 µm diameter tumor spheroids as described previously [19]. The plates were kept in the incubator and spheroids were observed at the indicated time points under a Nikon

ECLIPSE Ti confocal microscope. At the end of the experiment, plates were incubated with 0.1% Triton, 3.7% formaldehyde, Phalloidin-Rhodamin, and 400 ng/ml Hoechst for 48 hours at 4°C. Plates were washed three times with PBS, and imaged using a Nikon ECLIPSE Ti2 confocal microscope.

Random migration assay

96 well-plates were coated with collagen (50 µl/well, 20 µg/ml) 1 hour 37°C and washed with PBS. Cells were seeded into the coated 96-well plates at the density of 8000 cells/well overnight and stained with Hoechst (Thermo Fisher 33242) diluted 1:7500 for 45 minutes. Images were taken every 5 minutes on a Nikon TE confocal microscope for 12 hours, at two positions per well. Tracks were analyzed using NIS Elements software. For epidermal growth factor (EGF) stimulation, cells were seeded and cultured in collagen-coated 96-well plate overnight with serum free medium and 50 ng/ml EGF was added 1 hour before tracking cell migration.

Cell cycle analysis

Cell cycle analysis was performed with a Click-iT EdU Flow Cytometry Kit (Invitrogen). Cells were cultured with 50 µm 5-ethynyl-2-deoxyuridine (EdU) for 4 h and fixed and stained according to the manufacturers protocol for analysis on a BD FACS Canto II.

Colony formation assays

Cell survival was measured by colony formation assay. 450 cells were seeded into a well of 6-well plate after 4 days of doxycycline treatment. After 7 days, cells were fixed with 4% formaldehyde and stained with Giemsa. Images were analyzed by Image J (ColonyArea package).

Expression analysis in breast cancer cohorts

The Cancer Genome Atlas [20] (TCGA) and Metabric breast cancer datasets [21] were analyzed for copy number alterations of GRHL2 and correlation with overall survival using cBioPortal [22]. The KM plotter database was analyzed to evaluate the association of GRHL2 expression with overall survival of patients with different subclasses of breast cancer[23].

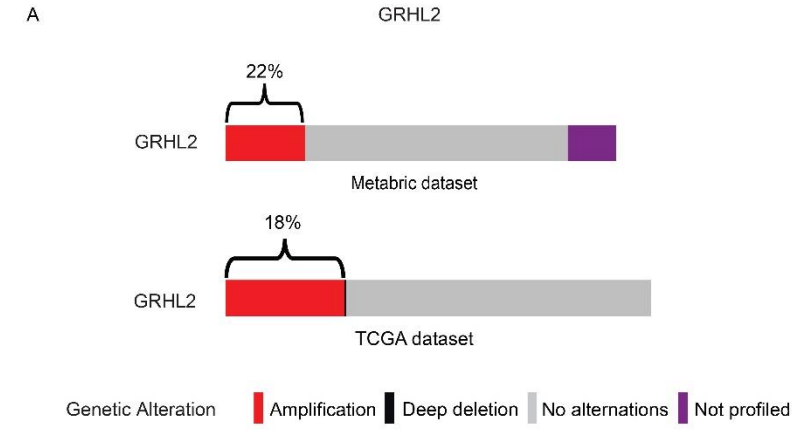
A
GRHL2
22%
GRHL2
Metabric dataset
18%
GRHL2
TCGA dataset
Genetic Alteration
Amplification
Deep deletion
No alternations
Not profiled

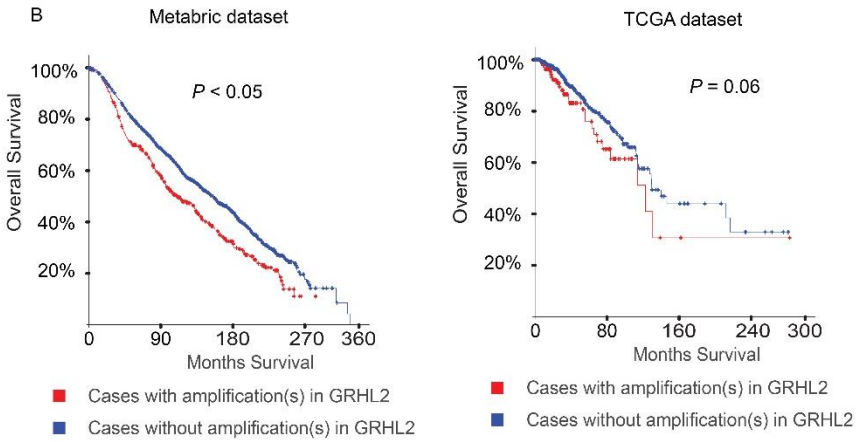
B
Metabric dataset
TCGA dataset
Overall Survival
P < 0.05
P = 0.06
Months Survival
Cases with amplification(s) in GRHL2
Cases without amplification(s) in GRHL2

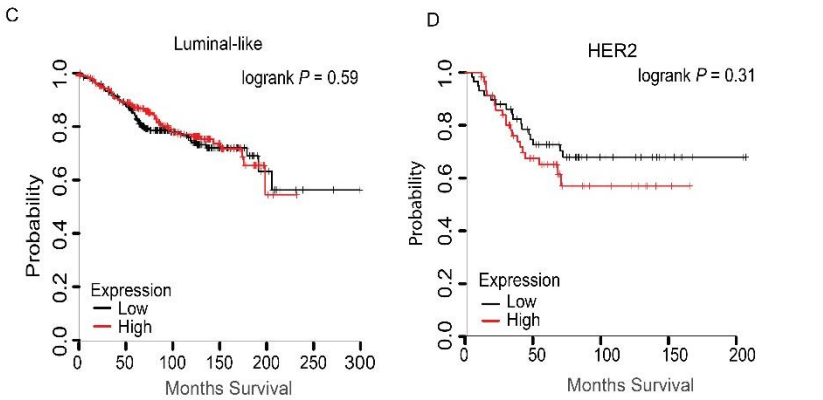
C
Luminal-like
logrank P = 0.59
D
HER2
logrank P = 0.31
Probability
Expression
Low
High
Months Survival

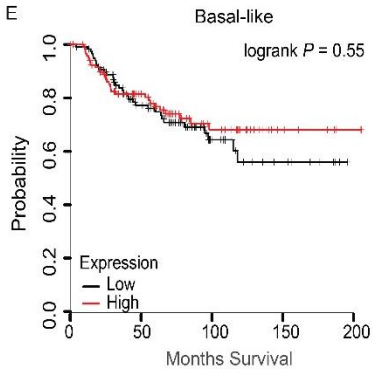
E
Basal-like
logrank P = 0.55
Probability
Expression
Low
High
Months Survival

(Last page) Fig. 1. GRHL2 expression in clinical breast cancer datasets. (A) Oncoprints showing *GRHL2* copy-number alternations from Metabric and TCGA datasets, generated by cBioPortal. **(B)** Kaplan-Meier survival analysis from Metabric and TCGA dataset, generated in cBioPortal. **(C-F)** Kaplan-Meier survival analysis for luminal (ER+) **(C)**, HER2-enriched **(D)**, and basal-like **(E)** subtypes of breast cancer, generated by KM plotter.

Statistical analyses

Statistical analyses were performed by GraphPad Prism 8. Details of statistical tests used are shown in the figure legends.

Results

GRHL2 is associated with poor prognosis but downregulated in basal B subtype breast cancer

In order to evaluate the clinical relevance of GRHL2 in breast cancer, GRHL2 alternations were examined in a series of published cohorts. *GRHL2* is located on chromosome 8q22.3, a genomic region that is frequently amplified or overexpressed in many cancers, including breast cancer and prostate cancer [16,24]. *GRHL2* gene amplification was detected in 22% to 18% of breast cancers (Fig. 1A). Kaplan-Meier survival analysis revealed that *GRHL2* gene copy number was associated with a trend toward a lower overall survival rate in patients with breast cancer although this was significant in a Metabric dataset but not in a TCGA dataset (Fig. 1B). We next explored the association of GRHL2 expression levels with overall survival in different breast cancer subtypes[25]. In luminal-like (ER+) breast cancers no association of GRHL2 expression with prognosis was found (Fig. 1C). In HER2-enriched breast cancer there was not significant association of high GRHL2 expression with poor prognosis (Fig. 1D). In basal-like breast cancer on the other hand, there was a slight trend that was not significant towards better prognosis for patients with higher GRHL2 levels (Fig. 1E).

Previous analysis of RNA-seq data organized for a large panel of human breast cancer cell lines showed that *GRHL2* was downregulated in the basal B subtype [12]. Our RNA-seq data further confirmed this finding (Fig. 2A and B). Notably, HCC1500 and SUM149PT may have been misclassified. SUM149PT has been classified as basal A or basal B subtype [8,26] and reported to contain different subpopulations, according to expression level of EpCAM and CD49f surface markers [27]. Likewise, HCC1500 cells

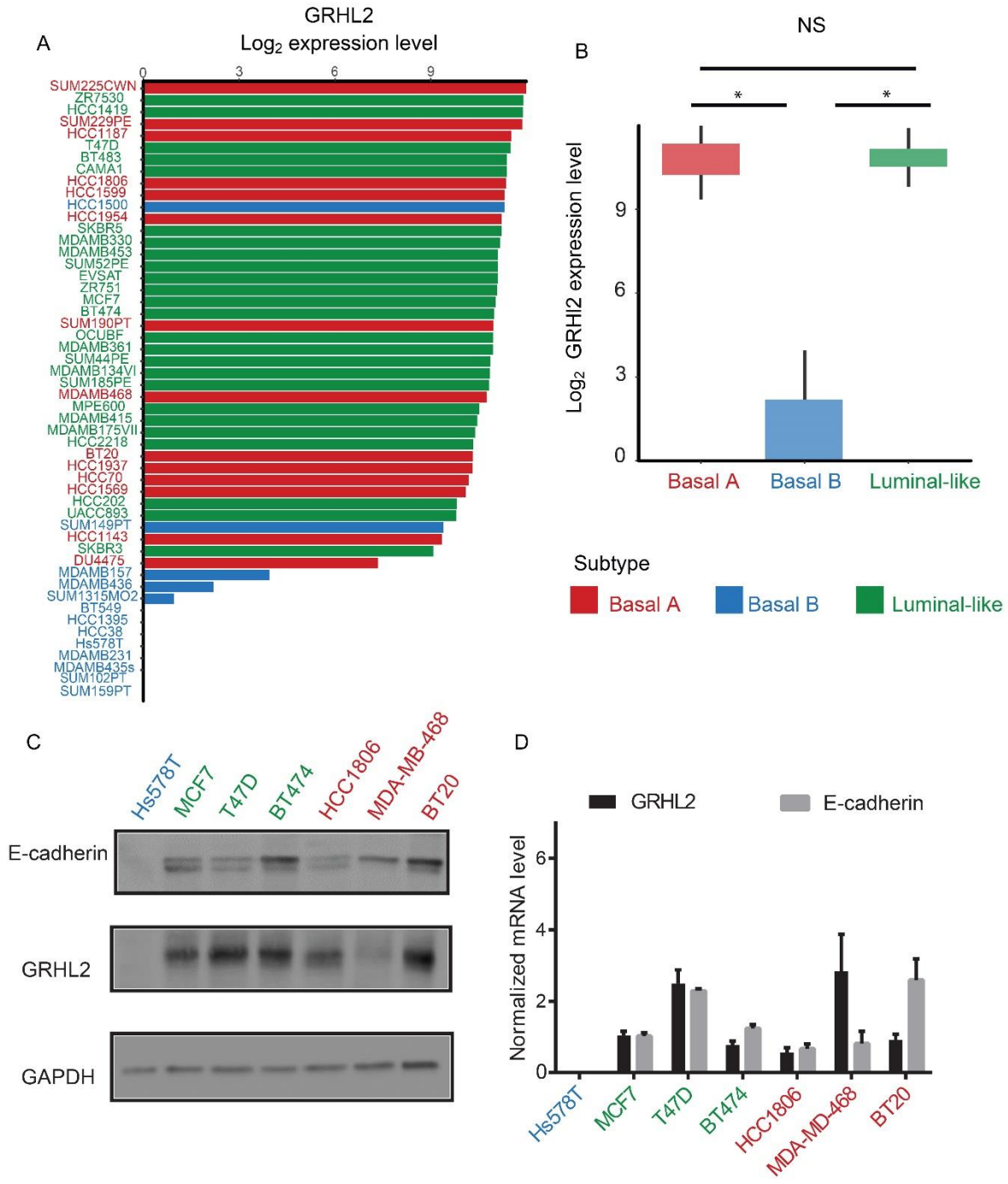

Fig. 2. GRHL2 expression in a panel of human breast cancer cell lines representing different subtypes. (A and B) *GRHL2* expression in a panel of >50 human breast cancer cell lines covering luminal-, basal A-, and basal B-like subtypes extracted from RNA-seq data. * indicates $p < 0.05$. Western blot analysis **(C)** and qRT-PCR **(D)** validating downregulation of GRHL2 and its target gene *CDH1* in basal B-like subtype breast cancer. Color codes refer to **B**

have been classified as basal A, due to a predominant population of cells that are positive for EpCAM and CD24 [3] or as basal B, owing to an enrichment for gene clusters associated with cancer stem cell- and invasive phenotypes [8]. To further validate

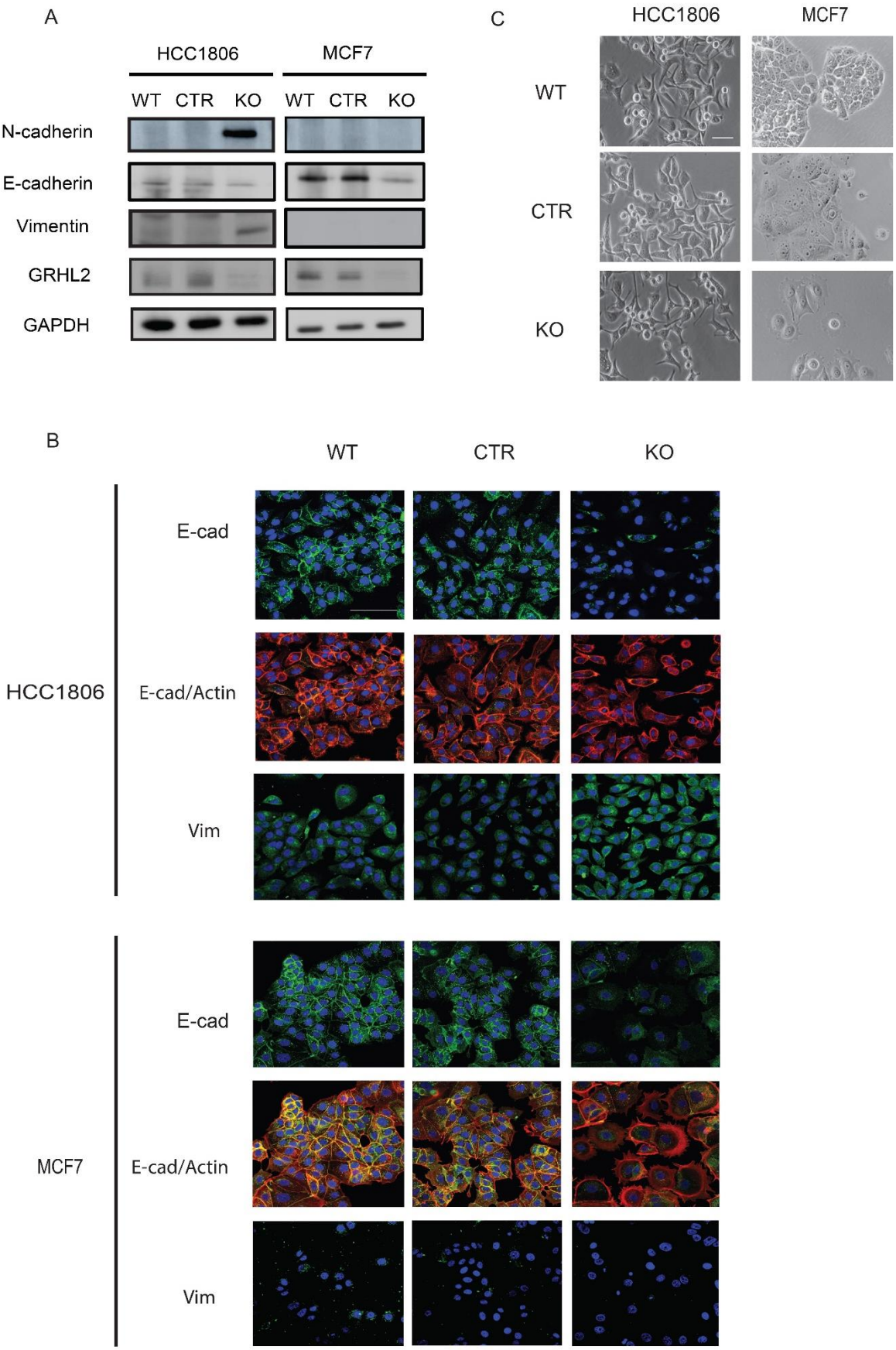
A
HCC1806
MCF7
WT CTR KO WT CTR KO
N-cadherin
E-cadherin
Vimentin
GRHL2
GAPDH
C
HCC1806
MCF7
WT
CTR
KO
B
WT
CTR
KO
HCC1806
E-cad
E-cad/Actin
Vim
MCF7
E-cad
E-cad/Actin
Vim

(Last page) Fig. 3. Response to GRHL2 knockout in luminal- and basal A-like cells – aspects of EMT. (A) Western blot analysis of the indicated proteins in wild type (WT) and sgCTR and sgGRHL2 transduced MCF7 and HCC1806 cells after 10 days doxycycline-induction. One experiment of two biological replicates is shown. **(B)** Immunofluorescence analysis of the indicated proteins in wild type (WT) and sgCTR and sgGRHL2 transduced MCF7 and HCC1806 cells after 10 days doxycycline-induction. One experiment of two biological replicates is shown. **(C)** Microphotographs showing morphology of wild type (WT) and sgCTR and sgGRHL2 transduced MCF7 and HCC1806 cells after 10 days doxycycline-induction. Scale bars in B and C, 100µm.

specific downregulation of GRHL2 in basal B, Western blot and qPCR were performed to detect GRHL2 protein and mRNA in a smaller panel of breast cancer cell lines. In agreement with the RNA-seq data, GRHL2 protein and mRNA were not detectable in Hs578T cells (basal B subtype), whereas it was expressed in basal A (HCC1806, MDA-MB-468 and BT20) and luminal-like (MCF7, T47D and BT474) subtypes (Fig. 2C and D).

E-cadherin (CDH1), a previously identified target gene of GRHL2, is a cell surface glycoprotein expressed in epithelial tissues that mediates cell-cell adhesion and is lost during EMT [14,28]. E-cadherin expression indeed correlated with GRHL2 expression and was not detectable in basal B subtype breast cancer, while basal A and luminal-like subtypes were positive for E-cadherin (Fig. 2C and D).

EMT and migratory responses to GRHL2 loss in luminal versus basal A-like breast cancer cells

Previous studies showed that loss of GRHL2 can be sufficient to trigger EMT [12]. We studied the response to GRHL2 loss in luminal and basal A-like cells using a conditional knockout approach. In both luminal (MCF7) and basal A-like cells (HCC1806) GRHL2 knockout, but not control sgRNA triggered a reduction in the epithelial marker, E-cadherin (Fig. 3A). However, the induction of mesenchymal markers, Vimentin and N-cadherin was only observed in HCC1806 cells. These Western blot results were confirmed using immunofluorescence. E-cadherin was expressed at cell–cell junctions and in the cytoplasm in HCC1806 and MCF7 cells and GRHL2 knockout led to reduced expression. A concomitant gain of Vimentin expression was only observed in HCC1806 cells (Fig. 3A and B). MCF7 cells showed reduced cell-cell contacts but still formed

islands and cells adopted a more flattened morphology whereas HCC1806 cells were more scattered in response to GRHL2 knockout (Fig. 3C).

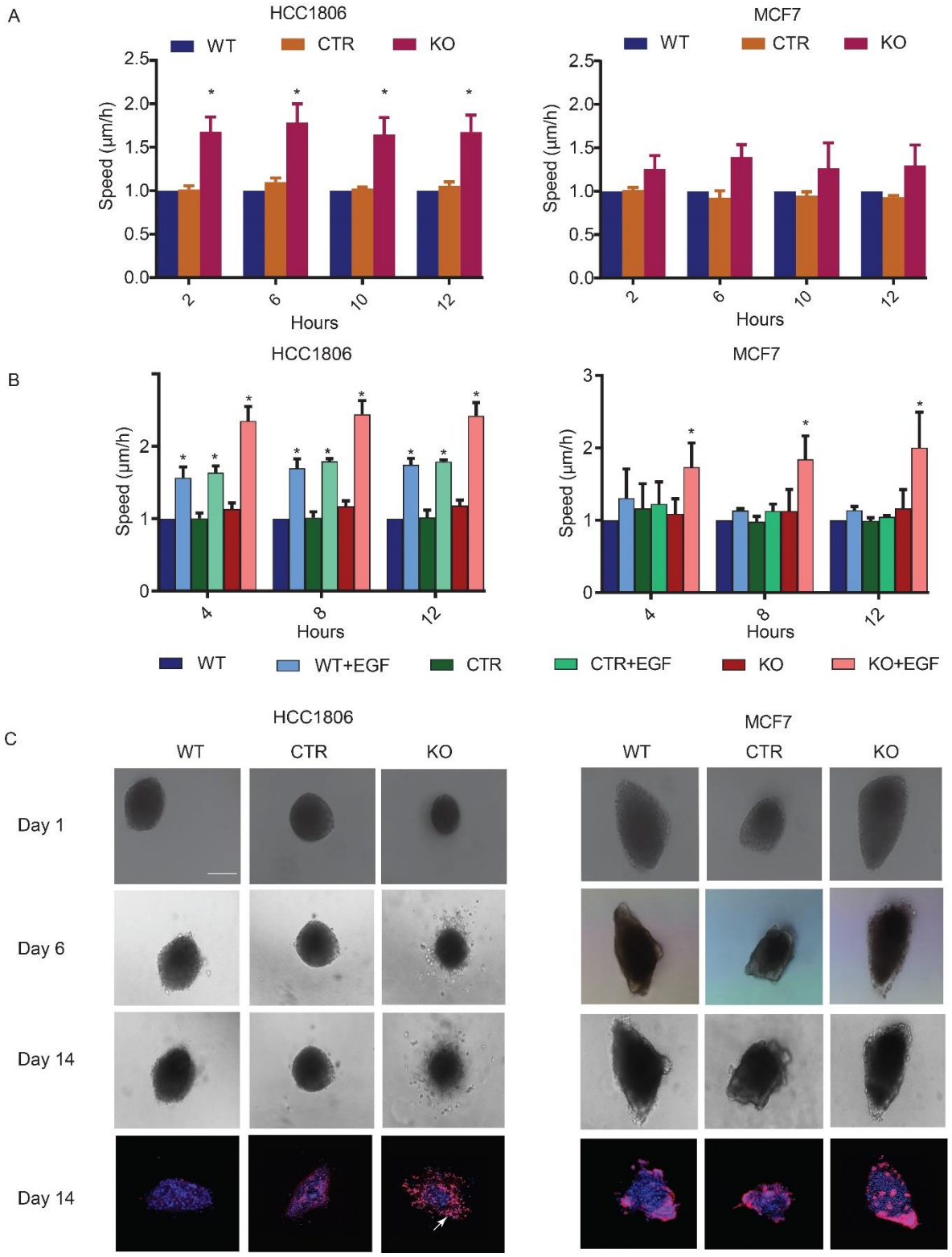

(Last page) Fig. 4. Response to GRHL2 knockout in luminal- and basal A-like cells – migratory behavior. (A) Analysis of random migration assay showing the average path speed (y-axis) captured at the indicated timepoints during the assay (x-axis) for wild type (WT) and sgCTR and sgGRHL2 transduced MCF7 and HCC1806 cells after 10 days doxycycline-induction. Data are presented as mean ± SEM from 3 biological replicates. Data are statistically analyzed by two-way ANOVA. * indicates $p < 0.05$. **(B)** Analysis of random migration assay showing the average path speed (y-axis) captured at the indicated timepoints during the assay (x-axis) for wild type (WT) and sgCTR and sgGRHL2 transduced MCF7 and HCC1806 cells after 10 days doxycycline-induction. Cells were left untreated or treated with 50 ng/ml EGF. Data are presented as mean ± SEM from 3 biological replicates. Data are statistically analyzed by two-way ANOVA. * indicates $p < 0.05$. **(C)** DIC (grey) and immunofluorescence images (blue, Hoechst; red, Rhodamin-Phalloidin) captured at the indicated timepoints after spheroid formation of collagen-embedded tumor spheroids derived from wild type (WT) and sgCTR and sgGRHL2 transduced HCC1806 and MCF7 cells after 10 days doxycycline-induction. Arrow shows invaded cells.

A shift from an epithelial to a mesenchymal phenotype is associated with enhanced migratory capability that may contribute to metastasis [31-33]. To investigate the effect of GRHL2 depletion on cell migration in HCC1806 and MCF7 cells, wild type, control sgRNA, and GRHL2 knockout cells were seeded into collagen-coated wells and intrinsic random migration was tracked. By calculating the mean square deviation (MSD) of the path length of each migrating cell, migration speed of the cells was determined. GRHL2 knockout led to an enhanced migration speed in HCC1806 cells whereas it did not significantly affect MCF7 cells (Fig. 4A).

EGF stimulates cell growth and migration in the mammary epithelium, by binding to the EGF receptor (EGFR) [34]. Previous studies showed that EGF promotes cell migration in basal B-like MDA-MB-231 cells [34]. We asked to what extent EGF-induced migration is modulated by GRHL2 loss and EMT status. EGF enhanced cell migration speed in HCC1806 cells and this effect was further increased upon GRHL2 loss (Figure 4B). By contrast, EGF failed to trigger cell migration in MCF7 but loss of GRHL2 resulted in enhanced cell migration in these cells.

Next, we investigated the effect of GRHL2 loss on the ability of luminal and basal A-like tumor spheroids to invade 3D extracellular matrix (ECM) scaffolds. MCF7 and HCC1806 tumor spheroids were generated in collagen matrices and invasion was analyzed over a 2-week period. Wild type and control sgRNA expressing HCC1806 spheroids did not show invasive behavior but GRHL2 knockout spheroids effectively

invaded into the surrounding collagen matrix (Fig. 4C). By contrast, MCF7 spheroids failed to invade the collagen matrix regardless of the presence or absence of GRHL2.

Together, these results indicate that loss of GRHL2 triggers several aspects associated with an EMT and leads to increased cell migration in basal A-like breast cancer cells whereas a partial EMT that enhances the response to EGF but does not lead to enhanced migratory potential per se, is induced in luminal-like breast cancer cells.

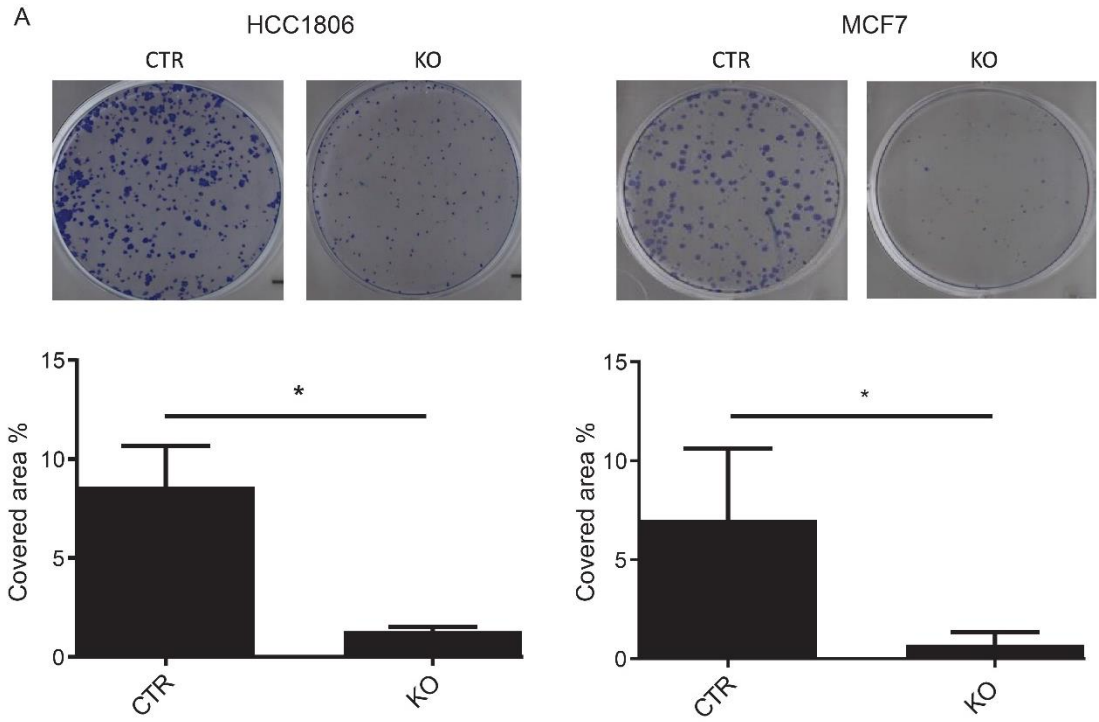

Fig. 5. Response to GRHL2 knockout in luminal- and basal A-like cells – colony formation capacity. Representative images and quantification of colony formation potential in control and GRHL2 depleted HCC1806 and MCF7 cells. Data are presented as mean ± SEM from 3 biological replicates. Data are statistically analyzed by t-test. * indicates $p < 0.05$.

Effects on growth triggered by GRHL2 loss in luminal versus basal A-like breast cancer cells

GRHL2 not only regulates genes involved in epithelial cell adhesion but also supports replication and growth of epithelial cells[2]. To address how GRHL2 loss affected the latter properties in luminal and basal A-like cells, colony formation assays were performed[35]. GRHL2 knockout caused a significant decrease in clonogenic cell survival in both HCC1806 and MCF7 cells (Fig. 5). However, after GRHL2 loss the area

A

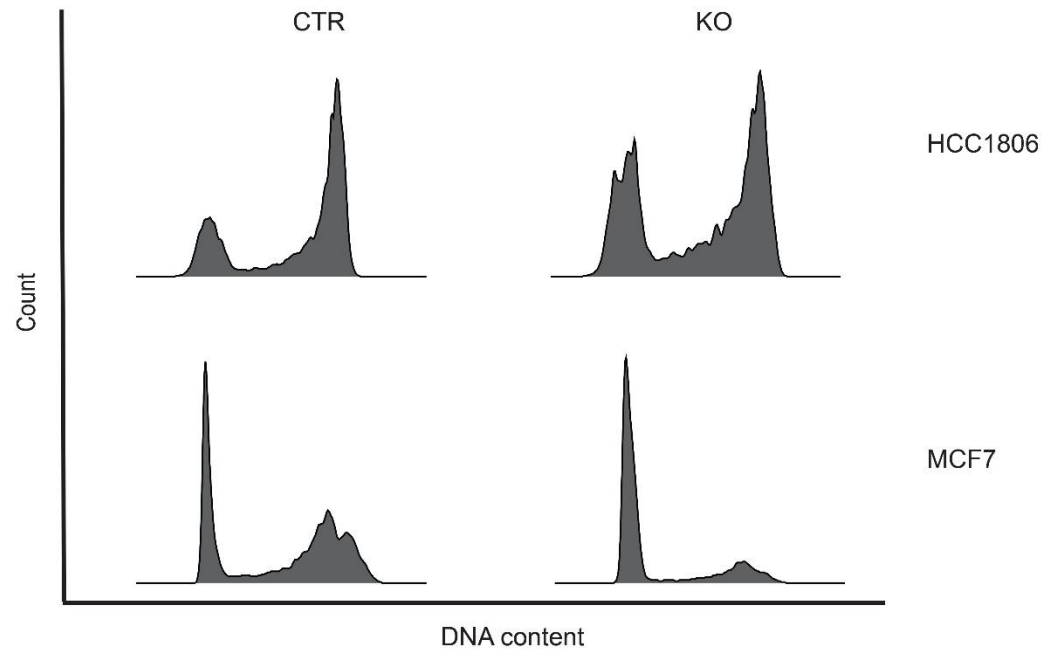

B

		CTR		KO		
		Mean	SEM	Mean	SEM	
HCC1806	G0/1	24.10%	0.80%	34.85%	0.21%	*
	S	11.25%	2.75%	12.40%	4.66%	
	G2	64.65%	3.55%	52.75%	3.45%	*

		CTR		KO		
		Mean	SEM	Mean	SEM	
MCF7	G0/1	46.00%	7.89%	76.57%	7.18%	*
	S	8.53%	1.77%	7.31%	3.81%	
	G2	44.33%	5.18%	15.57%	2.94%	*

C

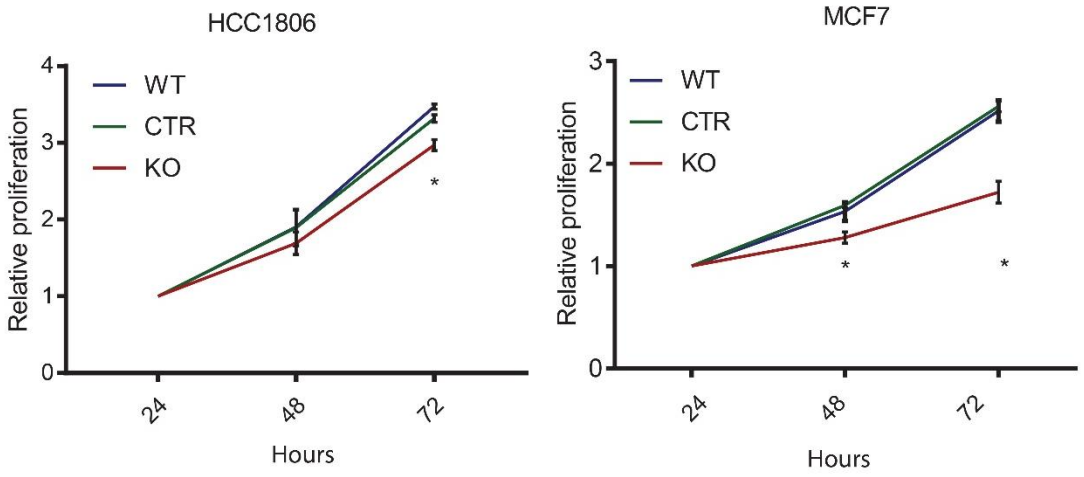

Fig. 6. Response to GRHL2 knockout in luminal- and basal A-like cells – proliferative capacity. (A and B) Representative FACS profiles (A) and quantification of cell cycle phase distribution

(B) in control and GRHL2 depleted HCC1806 and MCF7 cells. Data are presented as mean ± SEM from 2 and 3 biological replicates for MCF7and HCC1806, respectively. Data are statistically analyzed by t-test comparing KO to CTR cells. * indicates $p < 0.05$. **(C)** Graphs showing results from SRB assay for wild type (WT) and sgCTR and sgGRHL2 transduced MCF7 and HCC1806 cells after 4 days doxycycline-induction and subsequent incubation for the indicated time periods. Data are presented as mean ± SEM from 3 biological replicates. Data are statistically analyzed by t-test comparing CTR and KO to WT. * indicates $p < 0.05$.

covered by colonies in HCC1806 remained significantly higher than that in MCF7 cells. To address the effect of GRHL2 depletion on cell cycle progression, cell cycle analysis was performed. This demonstrated that a higher percentage of MCF7 cells were in G0/1 compared to HCC1806 and GRHL2 knockout resulted in a G0/1 arrest in MCF7 and a less-pronounced shift to G0/1 in HCC1806 cells (Fig. 6A and B).

To further address the effect of GRHL2 loss on proliferative potential, SRB assays were performed [36,37]. In agreement with the more robust block in colony formation and cell cycle progression observed in MCF7, GRHL2 knockout significantly inhibited cell proliferation of MCF7 cells at 2- and 3-days post seeding whereas a small but significant decrease in proliferation was observed at 3 days in HCC1806 (Fig. 6C).

We next examined candidate GRHL2-controlled genes that may underlie the observed distinct levels of suppression of cell proliferation in MCF7 and HCC1806 cells. GRHL2 has been shown to enhance expression of telomerase reverse transcriptase (TERT) in keratinocytes and oral squamous cell carcinoma cells [38,39], to support expression of proliferating cell nuclear antigen (PCNA) in colorectal cancer cells [40], and to suppress expression of the death receptor FAS in fibrosarcoma cells [24]. Expression of *FAS* was not significantly increased upon GRHL2 knockout in either cell type (Fig. 7). However, expression of *TERT* and *PCNA* mRNA was significantly downregulated in absence of GRHL2 in MCF7 whereas expression was unaltered or even increased in HCC1806 cells.

These results indicate that the impact of GRHL2 depletion on growth characteristics of different breast cancer subtypes may be distinct with luminal-like cells experiencing a robust growth arrest and basal A-like cells maintaining a reduced growth potential.

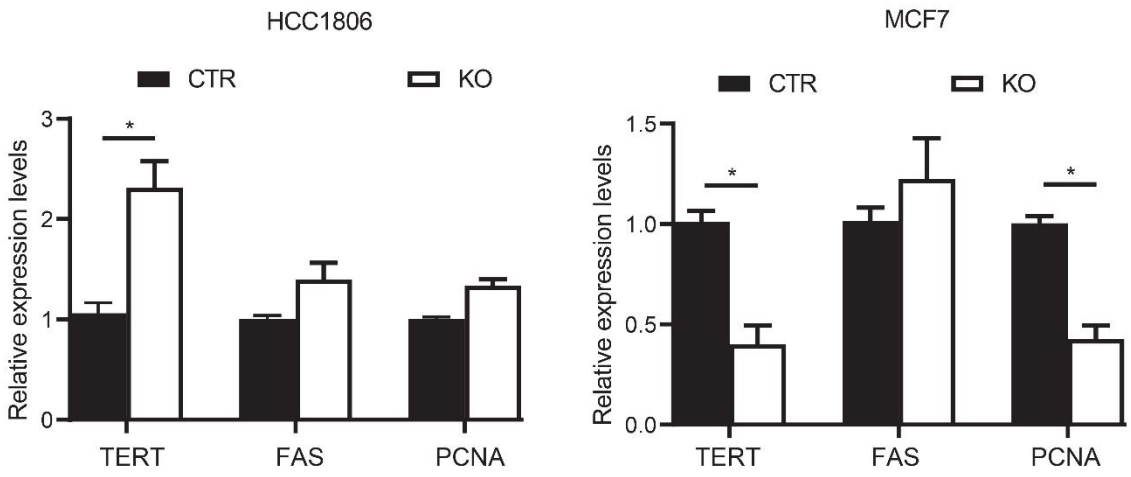

Fig. 7. Response to GRHL2 knockout in luminal- and basal A-like cells – changes in candidate target genes related to survival and proliferation. Graphs showing results from qRT-PCR assay for MCF7 and HCC1806 cells transduced with sgCTR and sgGRHL2 after 8 days doxycycline-induction. Data are statistically analyzed by t-test. Data are presented as mean ± SEM from 3 biological replicates. * indicates $p < 0.05$

Discussion

GRHL2 is located on chromosome 8q22 and amplified or overexpressed in several cancer types, including breast cancer [11,41]. *In vivo* and clinical studies support an oncogenic role of GRHL2 [11,16-18,42-44]. Our findings corroborate such a role for GRHL2 and demonstrate an association of GRHL2 expression with a trend toward poor prognosis in breast cancer. However, our results indicate that this association is different for different breast cancer subtypes, with a trend, albeit not significant, towards an association with better prognosis in the basal-like subtype. Our study using a panel of >50 human breast cancer cell lines, confirms and extends an earlier report showing that GRHL2 is downregulated in basal B-like breast cancer [12]. This is remarkable given its apparent relation to poor prognosis, since triple negative/basal-like tumors are often aggressive and have a poorer prognosis compared to the ER-positive luminal subtypes [4]. Moreover, basal B-like cells are enriched in EMT markers that are also associated with aggressiveness [4]. Indeed, GRHL2 may play a dual role in breast cancer [11,14,30]and a tumor- or metastasis-suppressive function has been related to its ability to suppress EMT, stemness, and invasion in cell line models and clinical samples [12,14,45]. The function of GRHL2 likely is context-dependent and the consequence of GRHL2 loss depends on the cancer type and the stage of cancer progression.

GRHL2 expression is associated with epithelial markers, including E-cadherin and claudins that are absent in basal B-like breast cancer cells. However, it is unknown whether luminal- and basal A-like breast cancer cells that have an epithelial phenotype with E-cadherin-mediated cell-cell contacts respond similarly to a loss of GRHL2. Our current study indicates that this response is modulated by the balance between a loss of growth stimulation and an induced EMT. This balance appears to be different for luminal and basal-like cells.

We find that expression of E-cadherin is downregulated in response to GRHL2 knockout in luminal-like and basal A-like breast cancer cells, consistent with previous studies [46-49]. However, we find that a further EMT-like shift is not necessarily induced. The acquisition of mesenchymal markers and enhanced cell migration and invasion is seen for HCC1806 (basal A) cells but not in MCF7 cells (luminal-like). These results demonstrate that the enhanced motile properties triggered by a loss of GRHL2 require acquisition of a mesenchymal phenotype. Loss of E-cadherin is not sufficient for enhanced cell migration and invasion of breast cancer cells [50]. The induction of mesenchymal markers, such as N-cadherin and Vimentin that we find to occur only in the HCC1806 cells may contribute to cell migration and invasion. N-cadherin junctions on the cell surface may act as migration tracks [51] and N-cadherin supports the organization of an actin network that drives cell migration [52]. Vimentin, a type III intermediate filament protein, is involved in cell adhesion, migration and signal transduction and emerges in pathologies processes involving epithelial cell migration [53]. Vimentin may facilitate cell migration through upregulation of AXL in breast cancer [54] but overexpression of Vimentin by itself does not enhance cell migration in MCF7 cells [55]. Altogether, our findings and other reports indicate that in order for GRHL2 loss to trigger a shift to a more motile behavior, loss of E-cadherin is not sufficient but a more elaborate transition is required, including loss of epithelial markers such as E-cadherin and gain of mesenchymal markers such as Vimentin and N-cadherin.

Our results show that loss of GRHL2 results in an inhibition of cell proliferation in basal-like and luminal-like breast cancer cells, consistent with earlier findings supporting an oncogenic role of GRHL2 [16,18,40]. However, we find that the impact is different for luminal and basal A-like cells with MCF7 cells experiencing a robust cell cycle and

growth arrest and HCC1806 maintaining a slow growth phenotype with a moderate increase in the fraction of cells in G0/1. This may result from the fact that GRHL2 is an integral part of ER transcriptional complex that induces expression of genes associated with cell proliferation in ER positive MCF7 cells only [11].No induction of cell death is observed in either cell type and expression of *FAS*, which was reported to be controlled by GRHL2, is unaltered [24]. *PCNA* expression is downregulated in MCF7 upon GRHL2, where a growth arrest is observed. Moreover, expression of *TERT*, which has been reported to be epigenetically controlled by GRHL2 [38,39] is attenuated in MCF7 but not HCC1806 following GRHL2 depletion indicating that replicative potential is differentially affected.

Taken together, our findings shed further light on the apparent dual role of GRHL2 in breast cancer. GRHL2 expression supports cell proliferation and suppresses cell motility in breast cancer cells but the outcome of GRHL2 loss differs for different subtypes. In luminal-like cells growth arrest is the main outcome of GRHL2 loss whereas in basal A-like cells reduced growth is accompanied by aspects of EMT and enhanced motility and invasion. This suggests that GRHL2 represents a candidate therapeutic target for luminal-like breast cancer, but interfering with GRHL2 expression or function is senseless in basal B-like breast cancers and may trigger unwanted effects in basal A-like breast cancers.

References

1 Harbeck, N. & Gnant, M. Breast cancer. *Lancet* **389**, 1134-1150, doi:10.1016/S0140-6736(16)31891-8 (2017).

2 Ma, L., Yan, H., Zhao, H. & Sun, J. Grainyhead-like 2 in development and cancer. *Tumour Biol* **39**, 1010428317698375, doi:10.1177/1010428317698375 (2017).

3 Keller, P. J. *et al.* Mapping the cellular and molecular heterogeneity of normal and malignant breast tissues and cultured cell lines. *Breast cancer research : BCR* **12**, R87, doi:10.1186/bcr2755 (2010).

4 Dai, X., Cheng, H., Bai, Z. & Li, J. Breast Cancer Cell Line Classification and Its Relevance with Breast Tumor Subtyping. *J Cancer* **8**, 3131-3141, doi:10.7150/jca.18457 (2017).

5 Dai, X. *et al.* Breast cancer intrinsic subtype classification, clinical use and future trends. *Am J Cancer Res* **5**, 2929-2943 (2015).

6 Tran, B. & Bedard, P. L. Luminal-B breast cancer and novel therapeutic targets. *Breast cancer research : BCR* **13**, 221, doi:10.1186/bcr2904 (2011).

7 Prat, A. *et al.* Clinical implications of the intrinsic molecular subtypes of breast cancer. *Breast* **24 Suppl 2**, S26-35, doi:10.1016/j.breast.2015.07.008 (2015).

8 Neve, R. M. *et al.* A collection of breast cancer cell lines for the study of functionally distinct cancer subtypes. *Cancer Cell* **10**, 515-527, doi:10.1016/j.ccr.2006.10.008 (2006).

9 Ming, Q. *et al.* Structural basis of gene regulation by the Grainyhead/CP2 transcription factor family. *Nucleic acids research* **46**, 2082-2095, doi:10.1093/nar/gkx1299 (2018).

10 Nüsslein-Volhard C., W. E., Kluding H. Mutations affecting the pattern of the larval cuticle inDrosophila melanogaster : I. Zygotic loci on the second chromosome. *Wilehm Roux Arch Dev Biol.* **193**, doi:10.1007/BF00848156. (1984).

11 Reese, R. M., Harrison, M. M. & Alarid, E. T. Grainyhead-like Protein 2: The Emerging Role in Hormone-Dependent Cancers and Epigenetics. *Endocrinology* **160**, 1275-1288, doi:10.1210/en.2019-00213 (2019).

12 Cieply, B. *et al.* Suppression of the epithelial-mesenchymal transition by Grainyhead-like-2. *Cancer Res* **72**, 2440-2453, doi:10.1158/0008-5472.CAN-11-4038 (2012).

13 Pifer, P. M. *et al.* Grainyhead-like 2 inhibits the coactivator p300, suppressing tubulogenesis and the epithelial-mesenchymal transition. *Mol Biol Cell* **27**, 2479-2492, doi:10.1091/mbc.E16-04-0249 (2016).

14 Werner, S. *et al.* Dual roles of the transcription factor grainyhead-like 2 (GRHL2) in breast cancer. *The Journal of biological chemistry* **288**, 22993-23008, doi:10.1074/jbc.M113.456293 (2013).

15 Garnis, C., Coe, B. P., Zhang, L., Rosin, M. P. & Lam, W. L. Overexpression of LRP12, a gene contained within an 8q22 amplicon identified by high-resolution array CGH analysis of oral squamous cell carcinomas. *Oncogene* **23**, 2582-2586, doi:10.1038/sj.onc.1207367 (2004).

16 Paltoglou, S. *et al.* Novel Androgen Receptor Coregulator GRHL2 Exerts Both Oncogenic and Antimetastatic Functions in Prostate Cancer. *Cancer Res* **77**, 3417-3430, doi:10.1158/0008-5472.CAN-16-1616 (2017).

17 Pan, X. *et al.* GRHL2 suppresses tumor metastasis via regulation of transcriptional activity of RhoG in non-small cell lung cancer. *Am J Transl Res* **9**, 4217-4226 (2017).

18 Faddaoui, A. *et al.* Suppression of the grainyhead transcription factor 2 gene (GRHL2) inhibits the proliferation, migration, invasion and mediates cell cycle arrest of ovarian cancer cells. *Cell Cycle* **16**, 693-706, doi:10.1080/15384101.2017.1295181 (2017).

19 Truong HH, X. J., Ghotra VP, Nirmala E, Haazen L, Le Dévédec SE, Balcioğlu HE, He S, Snaar-Jagalska BE, Vreugdenhil E, Meerman JH, van de Water B, Danen EH. β1 Integrin Inhibition Elicits a Prometastatic Switch Through the TGFb–miR-200–ZEB Network in E-Cadherin–Positive Triple-Negative Breast Cancer. *SCi Signal* (2014).

20 Ciriello, G. *et al.* Comprehensive Molecular Portraits of Invasive Lobular Breast Cancer. *Cell* **163**, 506-519, doi:10.1016/j.cell.2015.09.033 (2015).

21 Pereira, B. *et al.* The somatic mutation profiles of 2,433 breast cancers refines their genomic and transcriptomic landscapes. *Nature communications* **7**, 11479, doi:10.1038/ncomms11479 (2016).

22 Gao, J. *et al.* Integrative analysis of complex cancer genomics and clinical profiles using the cBioPortal. *Sci Signal* **6**, pl1, doi:10.1126/scisignal.2004088 (2013).

23 Gyorffy, B. *et al.* An online survival analysis tool to rapidly assess the effect of 22,277 genes on breast cancer prognosis using microarray data of 1,809 patients. *Breast Cancer Res Treat* **123**, 725-731, doi:10.1007/s10549-009-0674-9 (2010).

24 Dompe, N. *et al.* A whole-genome RNAi screen identifies an 8q22 gene cluster that inhibits death receptor-mediated apoptosis. *Proceedings of the National Academy of Sciences of the United States of America* **108**, E943-951, doi:10.1073/pnas.1100132108 (2011).

25 Holliday, D. L. & Speirs, V. Choosing the right cell line for breast cancer research. *Breast cancer research* **13**, 215 (2011).

26 Su, Y., Pogash, T. J., Nguyen, T. D. & Russo, J. Development and characterization of two human triple-negative breast cancer cell lines with highly tumorigenic and metastatic capabilities. *Cancer Med* **5**, 558-573, doi:10.1002/cam4.616 (2016).

27 Prat, A. *et al.* Characterization of cell lines derived from breast cancers and normal mammary tissues for the study of the intrinsic molecular subtypes. *Breast Cancer Res Treat* **142**, 237-255, doi:10.1007/s10549-013-2743-3 (2013).

28 Teo, K. *et al.* E-cadherin loss induces targetable autocrine activation of growth factor signalling in lobular breast cancer. *Sci Rep* **8**, 15454, doi:10.1038/s41598-018-33525-5 (2018).

29 Nieto, M. A., Huang, R. Y., Jackson, R. A. & Thiery, J. P. Emt: 2016. *Cell* **166**, 21-45, doi:10.1016/j.cell.2016.06.028 (2016).

30 Frisch, S. M., Farris, J. C. & Pifer, P. M. Roles of Grainyhead-like transcription factors in cancer. *Oncogene*, doi:10.1038/onc.2017.178 (2017).

31 Zhu, H. *et al.* The role of the hyaluronan receptor CD44 in mesenchymal stem cell migration in the extracellular matrix. *Stem cells (Dayton, Ohio)* **24**, 928-935, doi:10.1634/stemcells.2005-0186 (2006).

32 Xu, H. *et al.* The role of CD44 in epithelial-mesenchymal transition and cancer development. *OncoTargets and therapy* **8**, 3783-3792, doi:10.2147/OTT.S95470 (2015).

33 Lauffenburger, D. A. & Horwitz, A. F. Cell migration: a physically integrated molecular process. *Cell* **84**, 359-369, doi:10.1016/s0092-8674(00)81280-5 (1996).

34 Price, J. T., Tiganis, T., Agarwal, A., Djakiew, D. & Thompson, E. W. Epidermal growth factor promotes MDA-MB-231 breast cancer cell migration through a phosphatidylinositol 3'-kinase and phospholipase C-dependent mechanism. *Cancer Res* **59**, 5475-5478 (1999).

35 Franken, N. A., Rodermond, H. M., Stap, J., Haveman, J. & van Bree, C. Clonogenic assay of cells in vitro. *Nature protocols* **1**, 2315-2319, doi:10.1038/nprot.2006.339 (2006).

36 Orellana, E. A. & Kasinski, A. L. Sulforhodamine B (SRB) Assay in Cell Culture to Investigate Cell Proliferation. *Bio-protocol* **6**, doi:10.21769/BioProtoc.1984 (2016).

37 Vichai, V. & Kirtikara, K. Sulforhodamine B colorimetric assay for cytotoxicity screening. *Nature protocols* **1**, 1112-1116, doi:10.1038/nprot.2006.179 (2006).

38 Kang, X., Chen, W., Kim, R. H., Kang, M. K. & Park, N. H. Regulation of the hTERT promoter activity by MSH2, the hnRNPs K and D, and GRHL2 in human oral squamous cell carcinoma cells. *Oncogene* **28**, 565-574, doi:10.1038/onc.2008.404 (2009).

39 Chen, W. *et al.* Grainyhead-like 2 enhances the human telomerase reverse transcriptase gene expression by inhibiting DNA methylation at the 5'-CpG island in normal human keratinocytes. *The Journal of biological chemistry* **285**, 40852-40863, doi:10.1074/jbc.M110.103812 (2010).

40 Hu, F., He, Z., Sun, C. & Rong, D. Knockdown of GRHL2 inhibited proliferation and induced apoptosis of colorectal cancer by suppressing the PI3K/Akt pathway. *Gene* **700**, 96-104, doi:10.1016/j.gene.2019.03.051 (2019).

41 Mlacki, M., Kikulska, A., Krzywinska, E., Pawlak, M. & Wilanowski, T. Recent discoveries concerning the involvement of transcription factors from the Grainyhead-like family in cancer. *Experimental biology and medicine* **240**, 1396-1401, doi:10.1177/1535370215588924 (2015).

42 Yang, X., Vasudevan, P., Parekh, V., Penev, A. & Cunningham, J. M. Bridging cancer biology with the clinic: relative expression of a GRHL2-mediated gene-set pair predicts breast cancer metastasis. *PLoS One* **8**, e56195, doi:10.1371/journal.pone.0056195 (2013).

43 Quan, Y. *et al.* Downregulation of GRHL2 inhibits the proliferation of colorectal cancer cells by targeting ZEB1. *Cancer Biol Ther* **15**, 878-887, doi:10.4161/cbt.28877 (2014).

44 Butz, H. *et al.* Integrative bioinformatics analysis reveals new prognostic biomarkers of clear cell renal cell carcinoma. *Clinical chemistry* **60**, 1314-1326, doi:10.1373/clinchem.2014.225854 (2014).

45 Cieply, B., Farris, J., Denvir, J., Ford, H. L. & Frisch, S. M. Epithelial-mesenchymal transition and tumor suppression are controlled by a reciprocal feedback loop between ZEB1 and Grainyhead-like-2. *Cancer Res* **73**, 6299-6309, doi:10.1158/0008-5472.CAN-12-4082 (2013).

46 Chen, W. *et al.* Grainyhead-like 2 (GRHL2) knockout abolishes oral cancer development through reciprocal regulation of the MAP kinase and TGF-beta signaling pathways. *Oncogenesis* **7**, 38, doi:10.1038/s41389-018-0047-5 (2018).
47 Chen, W. *et al.* Grainyhead-like 2 regulates epithelial plasticity and stemness in oral cancer cells. *Carcinogenesis* **37**, 500-510, doi:10.1093/carcin/bgw027 (2016).
48 Chung, V. Y. *et al.* GRHL2-miR-200-ZEB1 maintains the epithelial status of ovarian cancer through transcriptional regulation and histone modification. *Sci Rep* **6**, 19943, doi:10.1038/srep19943 (2016).
49 Farris, J. C. *et al.* Grainyhead-like 2 Reverses the Metabolic Changes Induced by the Oncogenic Epithelial-Mesenchymal Transition: Effects on Anoikis. *Mol Cancer Res* **14**, 528-538, doi:10.1158/1541-7786.MCR-16-0050 (2016).
50 Sommers, C. L. *et al.* Cell adhesion molecule uvomorulin expression in human breast cancer cell lines: relationship to morphology and invasive capacities. *Cell growth & differentiation : the molecular biology journal of the American Association for Cancer Research* **2**, 365-372 (1991).
51 Shih, W. & Yamada, S. N-cadherin-mediated cell-cell adhesion promotes cell migration in a three-dimensional matrix. *J Cell Sci* **125**, 3661-3670, doi:10.1242/jcs.103861 (2012).
52 Ponti, A., Machacek, M., Gupton, S. L., Waterman-Storer, C. M. & Danuser, G. Two distinct actin networks drive the protrusion of migrating cells. *Science* **305**, 1782-1786, doi:10.1126/science.1100533 (2004).
53 Ivaska, J., Pallari, H. M., Nevo, J. & Eriksson, J. E. Novel functions of vimentin in cell adhesion, migration, and signaling. *Experimental cell research* **313**, 2050-2062, doi:10.1016/j.yexcr.2007.03.040 (2007).
54 Vuoriluoto, K. *et al.* Vimentin regulates EMT induction by Slug and oncogenic H-Ras and migration by governing Axl expression in breast cancer. *Oncogene* **30**, 1436-1448, doi:10.1038/onc.2010.509 (2011).
55 Sommers, C. L. *et al.* Loss of epithelial markers and acquisition of vimentin expression in adriamycin- and vinblastine-resistant human breast cancer cell lines. *Cancer Res* **52**, 5190-5197 (1992).

Acknowledgements

Zi Wang was supported by the China Scholarship Council and Bircan Coban was supported by the Dutch Cancer Society (grant no. 10967).

Author contributions

EHJD supervised the research. ZW and EHJD conceived, designed the experiments. ZW, BC, CYL and YJC performed the experiments. ZW and EHJD wrote the manuscript. All authors read, reviewed and approved the final manuscript.

Competing interests

The author(s) declare no competing interests.

Supplementary

Supplementary Table S1 RT-qPCR primers.

TERT	Forward	GATATCGTCCAGGCCCAGC
TERT	Reverse	CATGGACTACGTCGTGGGAG
FAS	Forward	GTGGACCCGCTCAGTACG
FAS	Reverse	TCTAGCAACAGACGTAAGAACCA
PCNA	Forward	GCCTGACAAATGCTTGCTGAC
PCNA	Reverse	TTGAGTGCCTCCAACACCTTC
GAPDH	Forward	CCATGGGGAAGGTGAAGGTC
GAPDH	Reverse	AGTTAAAAGCAGCCCTGGTGA